Supplementary Information (SI) for Chemical Science.

Materials and Methods

Acetone (high-performance liquid chromatography (HPLC) grade; Millipore Corp.), methanol (HPLC grade, Millipore Corp.), isopropyl alcohol (HPLC grade; Macron Fine Chemicals), toluene (HPLC grade; VWR Analytical), potassium hydroxide (99.97% purity; Acros Organics), and water (HPLC grade; VWR Analytical) were used as received. F:SnO_2-coated glass slides (FTO) (TEC 15, 12-15 Ω sq^{-1}; MSE Supplies) were cut into 2.5 cm x 1 cm substrates. Aqueous solutions of monodisperse polystyrene colloidal spheres (0.20 µm diameter, 2.7% w/w solids, 3% coefficient of variance [COV]; Polysciences Inc.) and monodisperse SiO_2 nanospheres (200 nm diameter, 10 mg mL^{-1} SiO_2 concentration, ≤ 12% COV; NanoComposix) were used as received.

Material Characterization: Scanning electron microscopy (SEM) images of photoelectrode structures were taken with a FEI Nova Nanolab 200 SEM. UV-vis absorption of thin films was measured on a Jasco V-780 spectrophotometer equipped with an integrating sphere. UV-Vis absorption spectra were calculated from transmission (T) and reflectance (R) spectra measured on the same sample [A (%) = 100% - T(%) - R (%)]. Powder x-ray diffraction measurements were performed using a Rigaku Miniflex II diffractometer.

Synthesis of omission glass structures: FTO substrates were cleaned by a sequential rinse in acetone, methanol, isopropanol, and water, followed by 30 minutes in a UV-ozone cleaner (Novascan) to remove surface organics and increase the hydrophilicity. Air annealing of substrates was performed in a muffle furnace equipped with a digital temperature controller (MTI Corp).

A stock solution of 200 nm SiO_2 was prepared by diluting the commercial solution to 2 mg mL^{-1} in water. A stock solution of 200 nm PS was prepared by diluting commercial stock solution to 1.05 mg mL^{-1} in water. These concentrations were chosen to give the same number of SiO_2 or PS spheres per volume of solution, accounting for their respective mass densities and equal diameters. Colloidal composite structures were deposited onto FTO substrates by the slow evaporation of mixture of the SiO_2 and PS solutions. This process induced the spheres to self-assemble into a close-packed composite with a random distribution of SiO_2 and PS spheres throughout the lattice.

The mixtures were prepared by combining the SiO_2 and PS stock solutions. The partial volume of each corresponded to the desired SiO_2:PS ratios and diluting with H_2O for a total of 5 mL suspension solution. All suspensions were prepared to have the same total concentration of spheres by number. For example, a 100% SiO_2 suspension was prepared by diluting the 2 mg mL^{-1} SiO_2 stock to 5 mL of total volume, giving a final mass concentration of 0.35 mg mL^{-1} SiO_2. A 100% PS suspension would be prepared by diluting the 1.05 mg mL^{-1} PS stock to 5 mL of total volume, giving a final mass concentration of 0.18 mg mL^{-1} PS. This enabled the fraction of each component in the self-assembled structure to be controlled simply by the relative fraction of each components' solution in the combined deposition solution.

To prepare an omission glass structure for a desired PS-SiO_2 ratio, a total of 5 mL of a mixed PS-SiO_2 solution was placed in a 20 mL high-density polyethylene scintillation vial. A single FTO substrate was positioned in each deposition vial at an angle of approximately 30° from vertical, with the FTO-coated side of the glass facing into the center of the vial. The self-assembly step was performed at 50 °C in a closed incubator until the solvent had evaporated (≥ 72 hours). This process resulted in the deposition of a uniform, close packed composite layer on the FTO-coated side of the substrate.

Synthesis of omission glass photoelectrodes: Metal oxide thin films were synthesized in an ALD reactor (GEMStar XT-D; Arradiance, Inc.). After the self-assembly of the colloidal composites completed, we deposited 50 cycles of ZnO (roughly 5 nm) in the ALD reactor at a deposition temperature of 85 °C. ZnO was grown from alternating exposures of diethylzinc (DEZ, 95%; Strem, Inc.) and H_2O (HPLC grade; VWR Analytical) precursors. Each cycle of ZnO growth had the following structure (at 20 sccm N_2 flow rate): 21 ms DEZ exposure, 1 s build-up step with the vacuum valve closed (to facilitate reactant access to the internal area of the omission glass structure), 30 s reactor purge under vacuum, 21 ms H_2O exposure, 1 s build-up, 30 s reactor purge. This ZnO growth was specific to the SiO_2 interfaces in the composite due to the absence of hydroxyl or other functional groups on the surface of PS that would seed the ALD growth process. This has the effect of binding the SiO_2 spheres together while leaving the PS ones relatively unaffected.[1] The ALD growth temperature (85 °C) was chosen to be lower than the glass transition temperature of polystyrene ($T_g \approx 97$ °C) to avoid sintering or distortion of the PS particles.[2] The low cycle number was chosen to minimize ZnO as an optical component in the overall electrode structure, as indicated by the negligible difference between the reflectance spectra before and after ZnO deposition (Figure 3). After ZnO deposition, we annealed the electrodes in air at 600 °C for 3 h (ramp rate 3 °C min^{-1} from room temperature), submerged the electrodes in toluene for 30 min, then exposed them to UV-ozone cleaning for 1 hr to ensure the complete removal of the PS nanospheres.

To form the photoelectrode on this structure, we deposited roughly 20 nm of TiO_2 (500 cycles of ALD growth at a reactor temperature of 150 °C), with the growth rate of 0.04 nm cycle^{-1} estimated from cross-sectional SEM.[3] TiO_2 was grown from alternating exposures of tetrakis(dimethylamido)titanium (TDMAT, 99%; Strem, Inc.) and H_2O precursors. Each cycle of TiO_2 growth had the following structure (at 20 sccm N_2 flow rate): 100 ms TDMAT exposure, 30 s reactor purge, 21 ms H_2O exposure, 30 s reactor purge. Finally, we annealed the photoelectrode in air at 500°C for 1 hr (ramp rate 3 °C min^{-1}) to crystallize the TiO_2 layer to the photoactive anatase phase on the omission glass photoanodes.

Photoelectrochemical characterization of the omission glass photoanodes: We characterized the photoelectrochemical properties of the omission glass photoanodes by cyclic voltammetry and chronoamperometry under illumination from a 365 nm LED (M365LP1; Thorlabs) with a collimating lens adapter used to generate a uniform illumination profile across an area larger than any electrode used here. This wavelength was chosen to characterize the photoelectrochemical properties of photoelectrodes based on TiO_2, as the corresponding energy ($E = 3.4$ eV) is slightly larger than the band gap of anatase TiO_2 ($E_g = 3.2$ eV). In all cases, the photoelectrodes of interest were characterized in a three-electrode configuration with a Pt mesh counter electrode and a Ag/AgCl reference electrode (saturated KCl; BASi). The three-neck flask used for these experiments was modified to include a large, flat quartz window to minimize unintended optical effects of the curved glass body. We measured the intensity of the LED illumination by placing an epoxy-protected photodiode (FDS-1010; Thorlabs) at the position of the electrode in water. The geometric area of each photoelectrode was defined by applying a layer of epoxy (Henkel Loctite EA 9460) around a uniform 0.04-0.08 cm^2 area in the structure. The epoxy was cured at room temperature for > 24 h prior to PEC characterization. We measured the geometric electrode areas using a high resolution (1200 dpi) flatbed scanner and the software package, ImageJ. All current densities were normalized to the geometric projected area of the electrode. For photoelectrochemical water oxidation experiments, we used an aqueous 0.1 M KOH solution as the electrolyte.

Finite Difference Time Domain (FDTD) Simulations: FDTD simulations were performed with the Python interface for the MIT Electromagnetic Equation Propagation (MEEP) open-source software package.[4] The voxel size of the Yee grid used in each of the FDTD simulations described here was 10 nm. The simulation volume was defined as a 3x3 supercell of a hexagonally close-packed array of 200 nm SiO_2 spheres (18 total in each layer). Each structure was 16 sphere layers tall. The percent omission was implemented by removing the target fraction of the spheres in the lattice at random. Unless otherwise noted, the remaining spheres were 'coated' with a 20 nm-thick layer of TiO_2 in the simulation via embedding a 200 nm SiO_2 sphere inside a TiO_2 sphere with a 240 nm diameter with the same centroid position. A 2D schematic of the simulation structure is shown in Figure S3a and a lattice with omitted spheres is shown in Figure S3b. The simulation volume was periodic in the x- and y-directions and terminated with perfectly matched layers (PML)[5] on the top and bottom of the z-dimension to implement transmission and reflection entirely away from the structure. Materials in the structure were represented by geometric primitives (spheres, slabs) with refractive index, n(λ), and extinction coefficient, k(λ), defined by reported literature values (Figure S4). The simulations were implemented in the time domain by initiating a smooth gaussian pulse chosen with a chosen central wavelength. Transmission and reflection at the central wavelength were measured at a plane just near the PMLs by the Fourier-transformed time domain fields accumulation method implemented in MEEP. Similarly, the steady-state components of the electric field vector were computed inside the volume of the electrode. The 3D absorption profiles were computed from the power dissipation in the dielectric material:

$$P(x, y, z) = -\frac{1}{2}\varepsilon_i(x, y, z)|E(x, y, z)|^2, \qquad (1)$$

where $\varepsilon_i(x,y,z)$ is the imaginary part of the dielectric constant as determined by the n and k values at that coordinate in the structure of the electrode. The transmission, reflectance, and absorption were computed for only the central wavelength of the pulse because n and k change over the range of wavelengths of interest in this work. Therefore, transmission and reflectance spectra were calculated with one simulation per wavelength of interest. The limited structure (e.g., location of the omissions) and periodic boundary conditions can produce simulation artifacts in single simulations that would not be representative of real materials. As a result, we averaged the results of repeated simulations (as indicated in the main text) to represent the characteristic properties of a disordered structure such as an omission glass with a degree of omission greater than 0%. This procedure generated computational reflectance and transmission spectra that were consistent with experimentally determined ones.

References

(1) Norman, M. A.; Perez, W. L.; Kline, C. C.; Coridan, R. H. Enhanced Photoelectrochemical Energy Conversion in Ultrathin Film Photoanodes with Hierarchically Tailorable Mesoscale Structure. *Advanced Functional Materials* **2018**, *28* (29), 1800481. https://doi.org/10.1002/adfm.201800481.

(2) Gigault, C.; Dalnoki-Veress, K.; Dutcher, J. R. Changes in the Morphology of Self-Assembled Polystyrene Microsphere Monolayers Produced by Annealing. *Journal of Colloid and Interface Science* **2001**, *243* (1), 143–155. https://doi.org/10.1006/jcis.2001.7885.

(3) Reed, P. J.; Mehrabi, H.; Schichtl, Z. G.; Coridan, R. H. Enhanced Electrochemical Stability of TiO2-Protected, Al-Doped ZnO Transparent Conducting Oxide Synthesized by Atomic Layer Deposition. *ACS Appl. Mater. Interfaces* **2018**, *10* (50), 43691–43698. https://doi.org/10.1021/acsami.8b16531.

(4) Oskooi, A. F.; Roundy, D.; Ibanescu, M.; Bermel, P.; Joannopoulos, J. D.; Johnson, S. G. Meep: A Flexible Free-Software Package for Electromagnetic Simulations by the FDTD Method. *Computer Physics Communications* **2010**, *181* (3), 687–702. https://doi.org/10.1016/j.cpc.2009.11.008.

(5) *Advances in FDTD Computational Electrodynamics: Photonics and Nanotechnology*; Taflove, A., Oskooi, A., Johnson, S. G., Eds.; Artech House antennas and propagation series; Artech House: Boston, 2013.

(6) Miikkulainen, V.; Leskelä, M.; Ritala, M.; Puurunen, R. L. Crystallinity of Inorganic Films Grown by Atomic Layer Deposition: Overview and General Trends. *Journal of Applied Physics* **2013**, *113* (2), 021301. https://doi.org/10.1063/1.4757907.

(7) Abendroth, B.; Moebus, T.; Rentrop, S.; Strohmeyer, R.; Vinnichenko, M.; Weling, T.; Stöcker, H.; Meyer, D. C. Atomic Layer Deposition of TiO2 from Tetrakis(Dimethylamino)Titanium and H2O. *Thin Solid Films* **2013**, *545*, 176–182. https://doi.org/10.1016/j.tsf.2013.07.076.

(8) Malitson, I. H. Interspecimen Comparison of the Refractive Index of Fused Silica. *J. Opt. Soc. Am., JOSA* **1965**, *55* (10), 1205–1209. https://doi.org/10.1364/JOSA.55.001205.

(9) Siefke, T.; Kroker, S.; Pfeiffer, K.; Puffky, O.; Dietrich, K.; Franta, D.; Ohlídal, I.; Szeghalmi, A.; Kley, E.-B.; Tünnermann, A. Materials Pushing the Application Limits of Wire Grid Polarizers Further into the Deep Ultraviolet Spectral Range. *Advanced Optical Materials* **2016**, *4* (11), 1780–1786. https://doi.org/10.1002/adom.201600250.

(10) König, T. A. F.; Ledin, P. A.; Kerszulis, J.; Mahmoud, Mahmoud. A.; El-Sayed, M. A.; Reynolds, J. R.; Tsukruk, V. V. Electrically Tunable Plasmonic Behavior of Nanocube–Polymer Nanomaterials Induced by a Redox-Active Electrochromic Polymer. *ACS Nano* **2014**, *8* (6), 6182–6192. https://doi.org/10.1021/nn501601e.

(11) Polyanskiy, M. N. Refractiveindex.Info Database of Optical Constants. *Sci Data* **2024**, *11* (1), 94. https://doi.org/10.1038/s41597-023-02898-2.

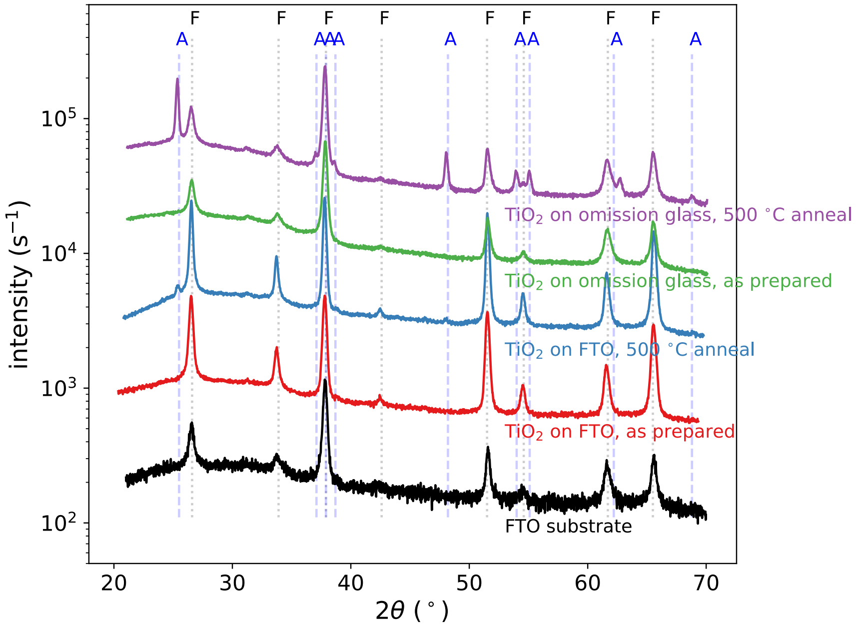

Figure S1 - XRD measurements (from bottom to top) of the FTO-coated substrate, a 500 cycle layer of TiO_2 on FTO as prepared by ALD, a 500 cycle layer of TiO_2 on FTO after 1 h anneal at 500 °C, a 500 cycle layer of TiO_2 on an omission glass photoelectrode as prepared by ALD, and a 500 cycle layer of TiO_2 on an omission glass photoelectrode after 1 h anneal at 500 °C. The dashed vertical lines indicate the positions for peaks for FTO (F) and anatase TiO_2 (A).

We characterized the phase of the as-prepared and air-annealed TiO_2 overlayer by XRD (Figure S1). The ALD process used here to deposit TiO_2 is known to yield an amorphous TiO_2 phase,[6,7] as indicated by the lack of observed peaks in the XRD data for the either of the as prepared samples other than those that match the Bragg reflections of the FTO substrate. New peaks were observed in the XRD measurements of the electrodes after annealing in air at 500 °C. These new peaks indexed to the Bragg reflections of anatase TiO_2, a photoactive phase of the compound. The XRD peaks for the anatase TiO_2 are more pronounced on the omission glass electrode due to the increased loading of TiO_2 in the porous structure compared to the planar one. Similarly, the substrate FTO peaks were obscured due to x-ray attenuation in the omission glass layer.

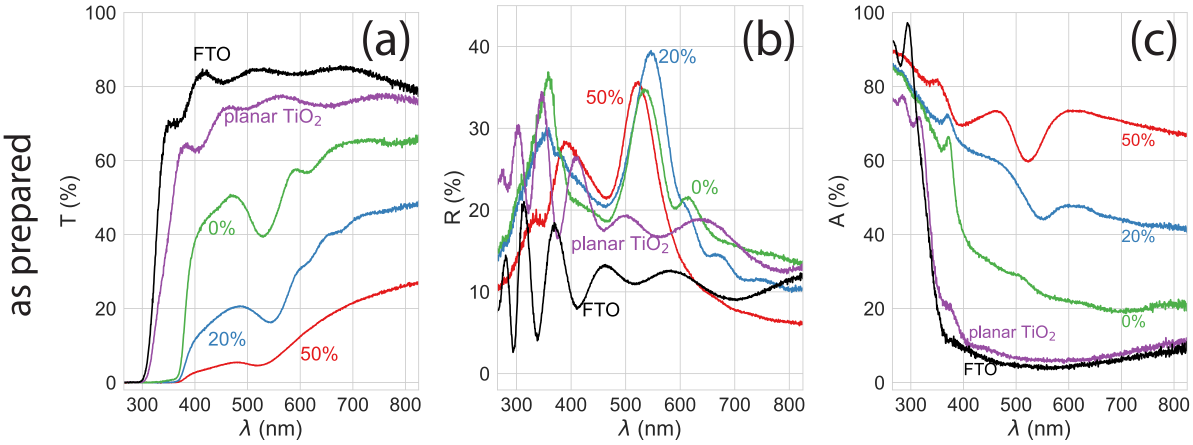

Figure S2 - UV-vis (a) transmission, (b) reflectance, and (c) absorption spectra of the as prepared 50% (red), 20% (blue) and 0% (green) omission glass electrodes shown in Figure 1. Absorption spectra of a planar, 20 nm TiO_2 layer (500 ALD cycles) on FTO (purple) and the FTO substrate (black) are included for comparison.

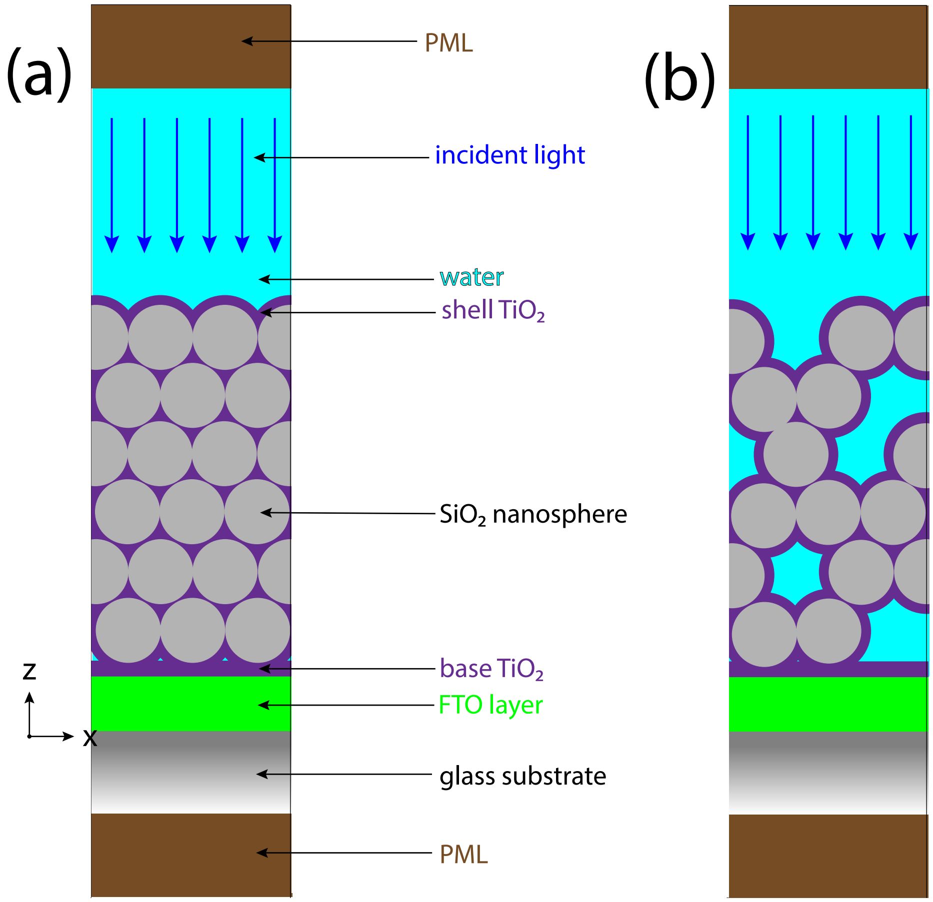

Figure S3 – (a) A schematic of the FDTD simulation geometry for a truncated photoelectrode structure (six layers rather than the sixteen used in the simulations shown here). (b) A schematic of the omission scheme used to represent the omission glass photoelectrode. The thickness of the electrodes used in these simulations was roughly 2.5 μm, which was smaller than the experimental electrodes (roughly 10-15 μm from scanning electron microscopy), though simulations and measurements showed that both structures were significantly opaque in practice.

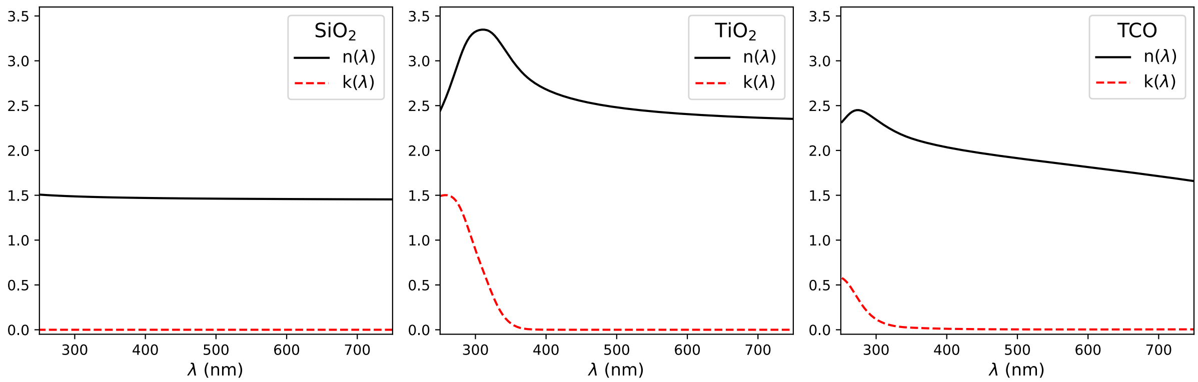

Figure S4 –Data used to represent the various materials used in the FDTD simulations. The wavelength-dependent refractive index, n(λ), and extinction coefficient, k(λ), for SiO_2,[8] TiO_2,[9] and a transparent conducting oxide[10] (Sn-doped In_2O_3) were taken from published measurements of each material. These data sets were taken from the collection *refractiveindex.info*, a publicly-available database of optical constants.[11]

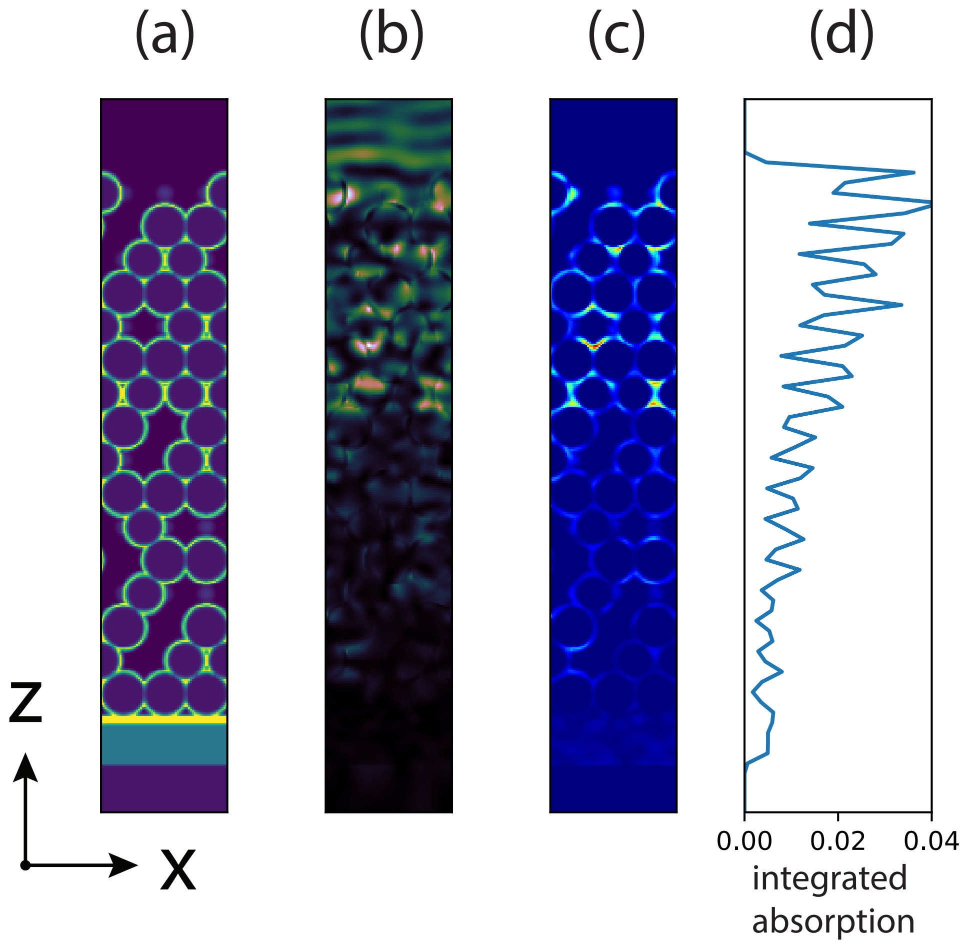

Figure S5 – Two-dimensional slices from an FDTD simulation of a 20% omission glass photoelectrode (λ = 365 nm). (a) The dielectric representation of the TiO_2 coating on SiO_2 spheres. Large values of ε are yellow while the water and SiO_2 is dark blue. The FTO layer is the green slab near the bottom of the figure. (b) The steady state distribution of $|E(x,y,z)|^2$. (c) The distribution of absorption, P(x,y,z). High absorption is red, while zero absorption is blue. (d) The integrated distribution of absorption in each voxel layer in the simulation.

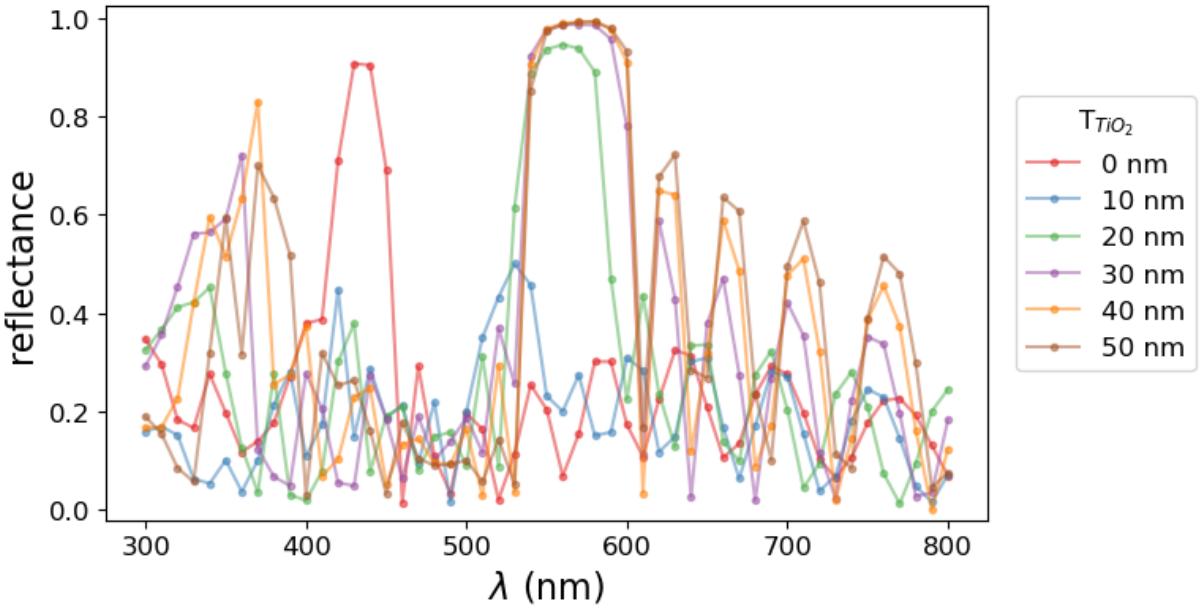

Figure S6 – FDTD simulations of the reflectance spectra for a 0% omission glass made from 200 nm SiO_2 spheres with increasing TiO_2 thickness (T_{TiO2}). As the void space between the spheres is infiltrated completely, the position and bandwidth of the reflectance stop band is fixed with increasing TiO_2 thickness.

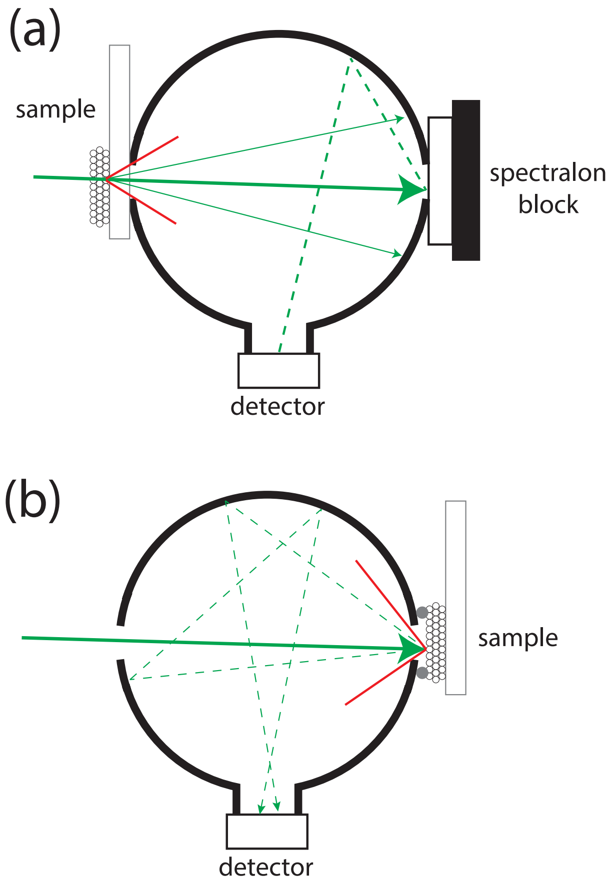

Figure S7 – Schematic diagrams representing the integrating sphere geometry for the (a) transmission and (b) reflectance measurements. The solid red lines indicate the angle of acceptance of the integrating sphere based on the thicknesses of the substrate (2.2 mm) in the transmission geometry and the o-ring offset (1 mm) in the reflectance geometry. The spectralon block in (a) closes the reflectance port at the back of the integrating sphere. The thicknesses of the offsets and the size of the ports on the integrating sphere result in an acceptance angle of greater than 150°.

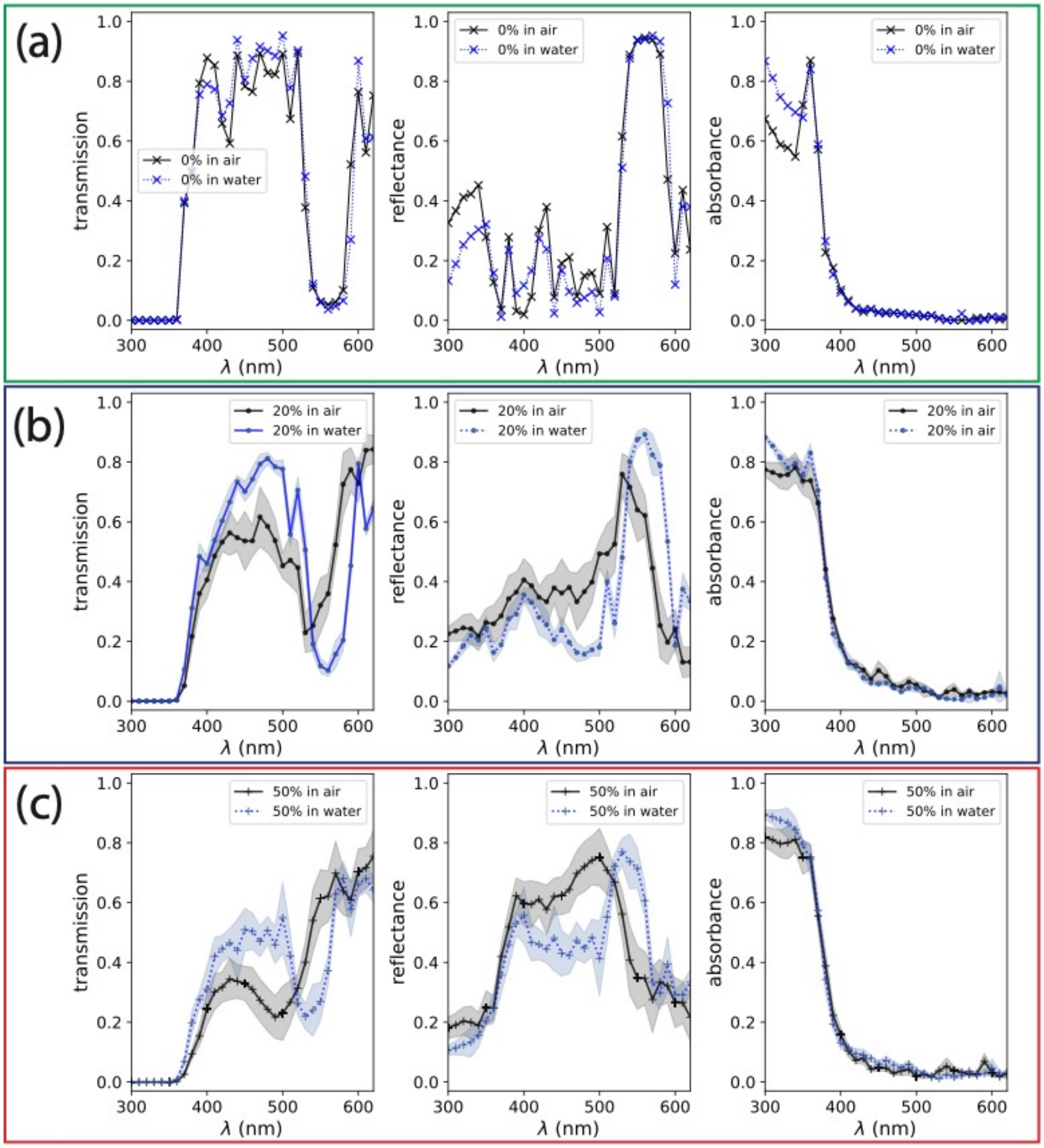

Figure S8 – Transmission, reflectance, and absorption spectra from FDTD simulations of (a) 0%, (b) 20%, and (c) 50% omission glass photoelectrodes in air (n = 1.0; black) and in water (n = 1.33; blue). The 20% and 50% omission glass spectra are computed from seven different structures, with the error bars computed from the standard deviation of each set of simulations.

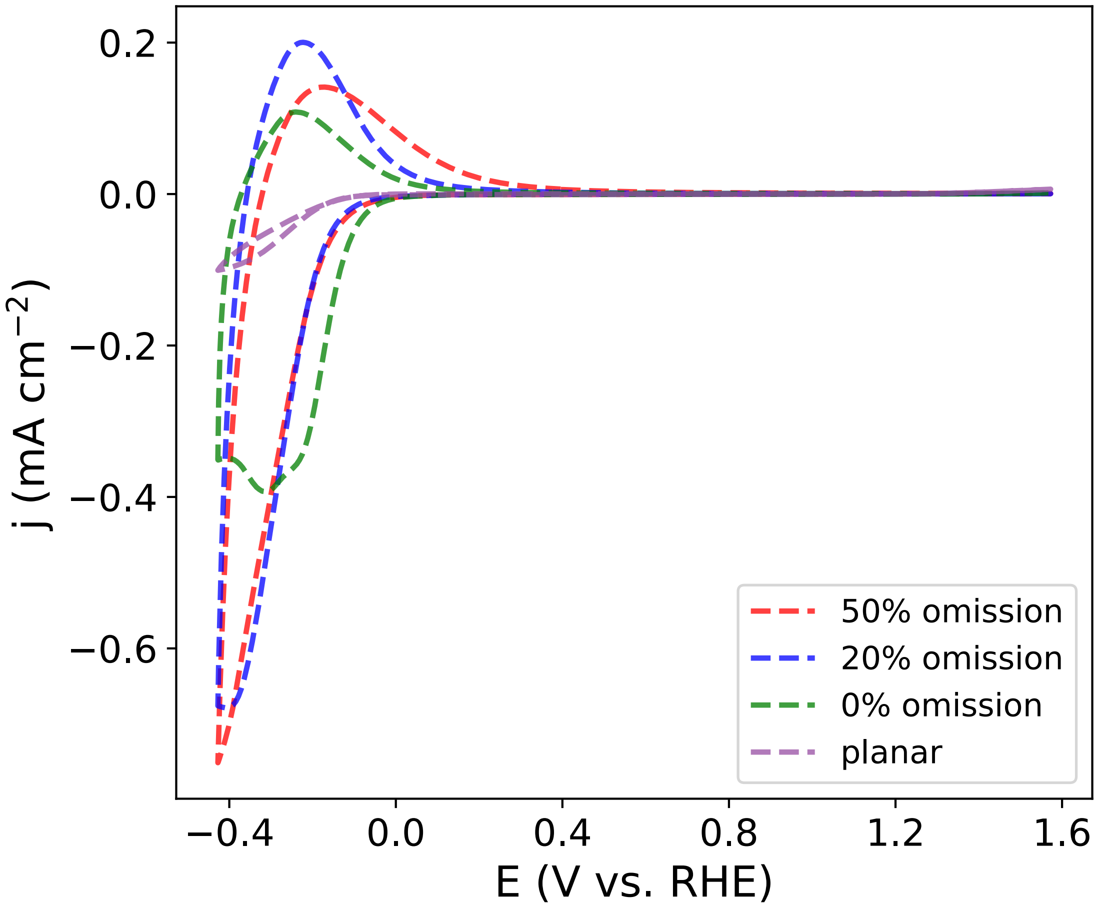

Figure S9 – *j-E* measurements from cyclic voltammetry (CV) for 50% (red), 20% (blue) and 0% (green) porous omission glass electrodes and a planar, annealed 20 nm TiO_2 electrode (purple) in 0.1 M KOH. The dashed line CV curves were measured in the absence of this illumination. These are the same dark scans as shown in Figure 7 in the main text, here isolated for improved view.

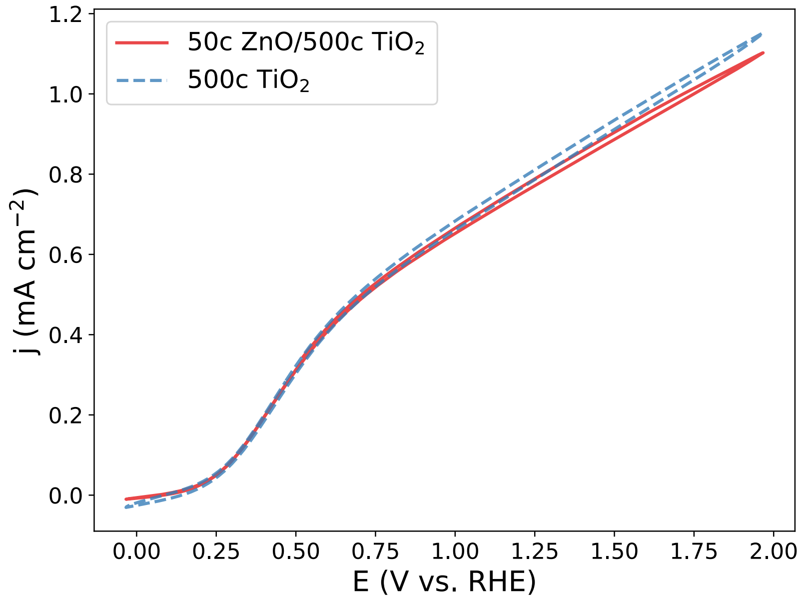

Figure S10 – Cyclic voltammetry comparing a planar, anatase TiO_2 photoanode (500 ALD cycles; blue dashed line) and a planar, anatase TiO_2 photoanode (500 c) with a 50 c ZnO interlayer. Each electrode layer was deposited on FTO-coated glass substrate. The measurements were performed in 0.1 M KOH under 1100 mW cm^{-2}, 365 nm LED illumination.

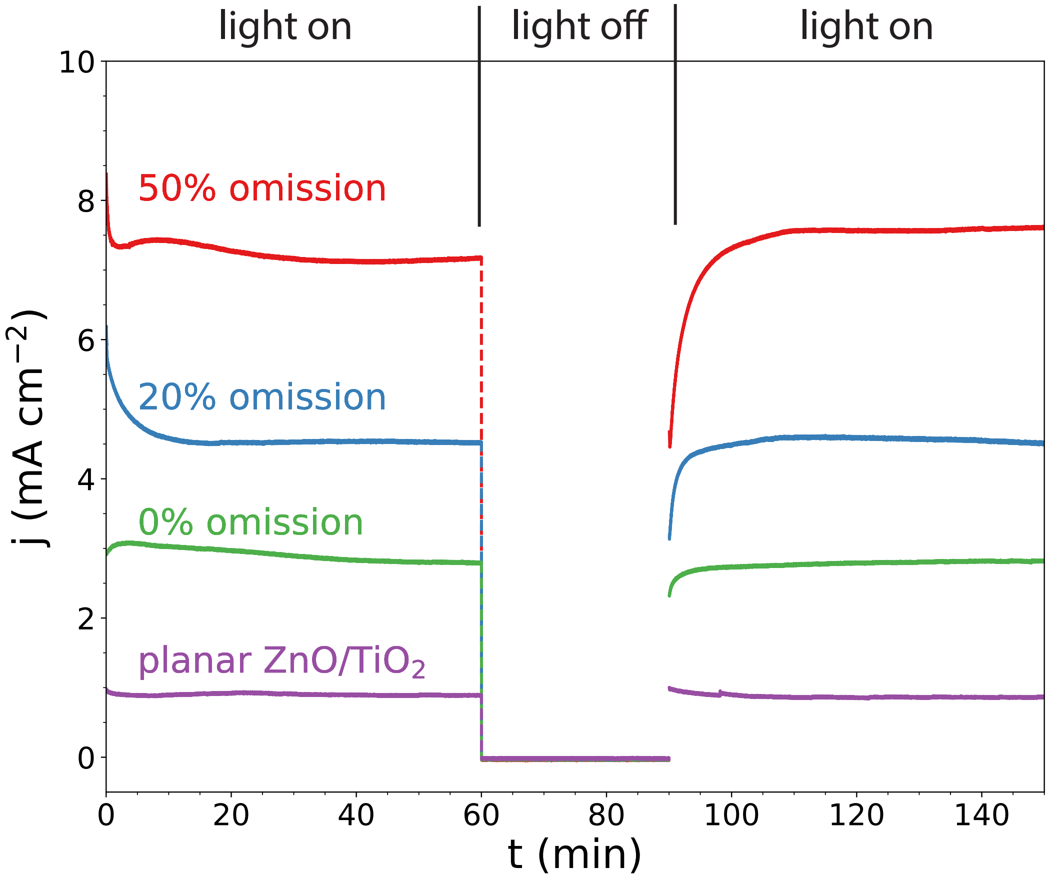

Figure S11 – Chronoamperometry (E = 1.71 V vs. RHE) measurements of photoelectrodes under 1100 mW cm^{-2}, 365 nm LED illumination in 0.1 M KOH. The LED was on for 60 minutes ('light on'), then turned off for 30 minutes ('light off'), and then back on for 60 minutes.